Highly Fluorescent Silica-Coated Bismuth-Doped Aluminosilicate Nanoparticles for Near-Infrared Bioimaging

ARTICLE *in* SMALL · JANUARY 2011

Impact Factor: 8.37 · DOI: 10.1002/smll.201001011 · Source: PubMed

11 AUTHORS, INCLUDING:

Yufang Zhu
University of Shanghai for Science and Tec…
67 PUBLICATIONS **2,805** CITATIONS
SEE PROFILE

Takayuki Asahara
Tokai University
500 PUBLICATIONS **32,677** CITATIONS
SEE PROFILE

Masaaki Ii
Osaka Medical College
80 PUBLICATIONS **3,459** CITATIONS
SEE PROFILE

Zhenhua Bai
University of South Carolina
20 PUBLICATIONS **204** CITATIONS
SEE PROFILE

small NANO MICRO

Bioimaging

Highly Fluorescent Silica-Coated Bismuth-Doped Aluminosilicate Nanoparticles for Near-Infrared Bioimaging

Hong-Tao Sun, Junjie Yang, Minoru Fujii, Yoshio Sakka, Yufang Zhu, Takayuki Asahara, Naoto Shirahata, Masaaki Ii, Zhenhua Bai, Ji-Guang Li, and Hong Gao*

For in vivo and deep-tissue imaging, near-infrared (NIR)-emitting nanoparticles (NPs) offer many advantages over visible-light-emitting NPs because the optical absorption and light scattering of biological media and tissue autofluorescence are minimal in the NIR region of the electromagnetic spectrum.[1] Up to now, a wide array of novel nanomaterials, including quantum dots (QDs), organic dyes, and dye-doped or undoped inorganic NPs, have been developed for bioimaging.[1–6] For instance, QDs modified with tumor-targeting ligands have been successfully used as in vivo cancer-targeted imaging agents of living animals.[2b] Unfortunately, most QDs contain extremely toxic elements such as cadmium and lead, and dyes are easily photobleached, which makes it rather difficult to use them for in vivo imaging in humans.[1–7] Consequently, the development of nontoxic and biocompatible NPs emitting in the NIR region, especially in the second biological window (1.0–1.4 μm), is urgently needed.[1]

Bismuth, atomic number 83 and the heaviest stable element in the periodic table, was established as an element in 1739 by Potts and Bergmann.[8a] Bismuth has long been associated with medicine.[8b] The earliest use of bismuth compounds in medicine appears to have been in the Middle Ages. Since the last century, various bismuth compounds have been used to treat syphilis, hypertension, infections, skin conditions, and gastrointestinal disorders.[8c,d] The recommended oral dosage for different bismuth salts is 100–450 mg, 3–4 times a day for several days/weeks.[9] It is well known that bismuth can exist in materials in different valence states, such as 0, +1, +2, +3, and +5, or even mixed valence states of +1 and +5; among them, the +3 state is the most stable form.[10] The diverse valence state of bismuth makes it promising for optically active centers in a wide range of applications, such as visible and NIR photonics.[10] However, to the best of our knowledge, bismuth-doped photonic materials have never been used for bioimaging.

Aluminosilicates are composed of aluminum, silicon, and oxygen, and are a major component of clay minerals. The use of aluminosilicates as biomedical materials has a long history; the ingestion of some aluminosilicates, such as zeolites, is considered to be analogous to eating clay since their main components are Si, Al, and O.[11] Recent results revealed that microporous aluminosilicate NPs have great potential for drug-delivery systems.[12,13] However, until now, there has been little effort to engineer aluminosilicates for bioimaging.

Herein, we demonstrate that the combined advantages of bismuth and aluminosilicates lead to a new type of nanosized biolabel, that is, NIR-emitting, silica-coated, bismuth-doped aluminosilicate NPs (Bi-AS-NPs), which are simple to prepare and exhibit highly efficient fluorescence covering the second biological window, high photostability, low cytotoxicity, and easy penetration into living tissues. Such NPs are fabricated based on a well-controlled phase transition from a bismuth-doped Fau/LTA nanozeolite mixture to amorphous NPs, followed by a simple sol–gel reaction with a silica source, tetraethyl orthosilicate (TEOS), at room temperature to form a silica layer on the surface of Bi-AS-NPs. Furthermore, we also show that the ultrastable and long-lived NIR photoluminescent (PL) emission from these NPs gives them great potential for in vivo PL and lifetime imaging in the optimal biological window (1000–1400 nm).

As shown in **Figure 1**a,b, the as-prepared zeolites, with good crystallinity, are composed of Faujasite (Fau) and Linde Type A (LTA) nanocrystals and have a broadly distributed particle size of 53 ± 25 nm, with a few over 100 nm (see Supporting Information, Figure S1). After removal of the tetramethylammonium (TMA) cation organic template at 580 °C, the crystalline structures were well retained. Bi-AS-NPs were obtained by annealing the bismuth-doped zeolites at 870 °C in an Ar atmosphere (Figure 1c). Energy-dispersive X-ray

Dr. H.-T. Sun, Dr. Y. Zhu, H. Gao
International Center for Young Scientists (ICYS)
National Institute for Materials Science (NIMS)
1-2-1 Sengen, Tsukuba-city, Ibaraki 305–047, Japan
E-mail: timothyhsun@gmail.com

J. Yang, Prof. T. Asahara, Dr. M. Ii
Institute of Biomedical Research and Innovation/RIKEN Center for Developmental Biology
Kobe 650–0047, Japan

J. Yang
Division of Cardiovascular Surgery
Department of Surgery
Osaka University Graduate School of Medicine
Osaka 565–0871, Japan

Prof. M. Fujii, Z. Bai
Department of Electrical and Electronic Engineering
Kobe University
Kobe 657–8501, Japan

Prof. Y. Sakka, Dr. N. Shirahata, Dr. J.-G. Li
Nano Ceramics Center
National Institute for Materials Science (NIMS)
1-2-1 Sengen, Tsukuba-city, Ibaraki 305–0047, Japan

DOI: 10.1002/smll.201001011

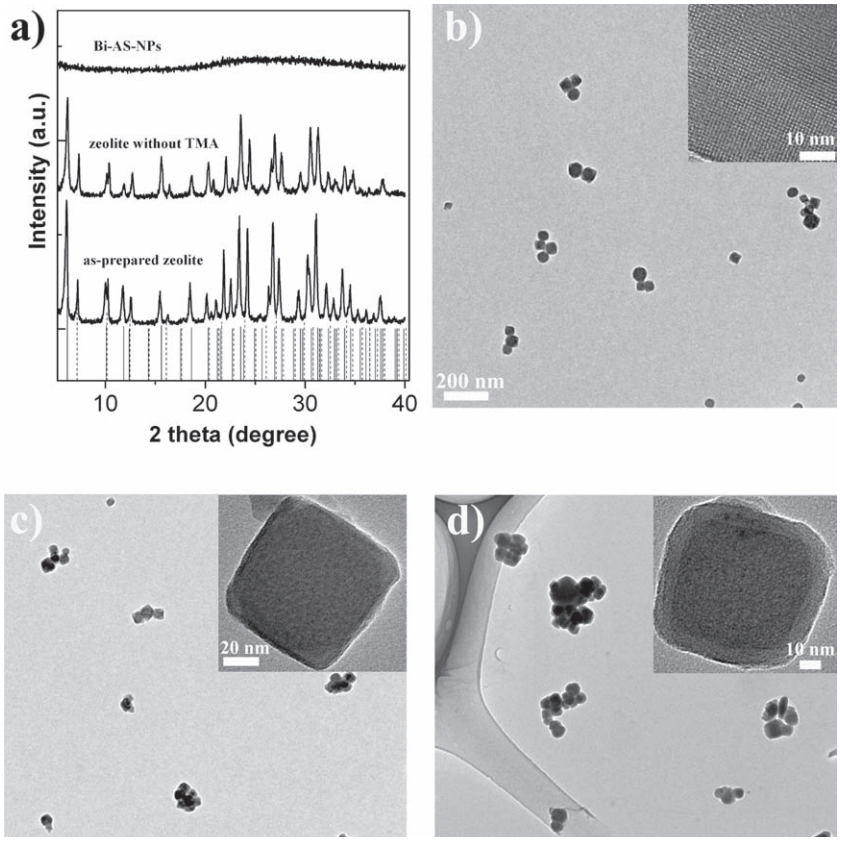

Figure 1. a) X-ray diffraction spectra of the as-prepared zeolites, zeolites removed from the template, and Bi-AS-NPs. The solid and dotted vertical lines represent the diffraction peaks of Fau and LTA zeolites, respectively. b–d) Transmission electron microscopy (TEM) images of b) the as-prepared zeolites, c) Bi-AS-NPs, and d) silica-coated Bi-AS-NPs.

spectroscopy (EDS) confirmed that the amorphous particles are composed of Si, Al, Bi, Na, and O (Supporting Information, Figure S2). Figure 1d clearly shows that NPs are encapsulated by a thin SiO_2 shell with a thickness of ≈9 nm. The ratio of the concentrations of NPs and TEOS was optimized to prevent the homogeneous nucleation of silica and to control the silica-shell thickness of the core/shell NPs (Supporting Information, Figure S3). The SiO_2 coating results in a higher surface potential (–51.07 mV) of NPs in comparison to the –42.64 mV of uncoated ones, which suggests that it is helpful to enhance the dispersibility of NPs in assay buffers.

Next, we thoroughly characterized the optical properties of the core/shell NPs. The NPs display two broad absorption bands covering the visible and NIR regions (**Figure 2**a), which can be assigned to the electronic transitions of Bi-related infrared-active centers (BiRIACs).[10] The NIR emissions of the core/shell NPs, under excitation at 514.5 and 690 nm, appear at 930–1560 nm (Figure 2b), and excitation bands occur not only in the visible range of 300–650 nm but also in the NIR region of 650–800 nm (Supporting Information, Figure S4). It is worth noting that the shape of the PL strongly depends on the excitation wavelength, which was also observed in other Bi-doped NIR-emitting materials.[10a–c] Recent results suggested that subvalent bismuth ions, that is, Bi^+ with the $6s^26p^2$ configuration, are the BiRIACs.[10a,b] Owing to the extended nature of the 6p orbitals, the crystal field also plays an important role in the luminescence properties. Thus, the excitation-wavelength-dependent infrared luminescence may be attributed to site-to-site variations in the environment of the emission centers. Examination of the PL decay curve found that the NPs show an effective lifetime of 232 μs (Figure 2c), which is much longer than those of most semiconductor QDs and traditional dyes.[14,15] The quantum efficiency (QE) of the NPs dispersed in phosphate-buffered saline (PBS) solution is as high as 14.6%. In addition, these NPs exhibit greater photostability than fluorescein or the well-known NIR cyanine fluorophores Cy5.5 and Cy7 (Figure 2d).[3] Clearly, the excitation and emission properties suggest that these NPs are suitable for in vivo NIR imaging.

Figure 3 shows the in vitro cytotoxicity effects of the core/shell NPs on HeLa and NIH3T3 cells after 24 h of exposure to increasing doses of silica-coated Bi-AS-NPs, as evaluated with the MTT assay (MTT = 3-(4,5-dimethylthiazol-2-yl)-2,5-diphenyltetrazolium bromide). It can be seen that the NPs do not show notable adverse effects on HeLa and NIH3T3 cell viability in concentrations up to 10 and 20 μg mL^{-1}, respectively. Even at a higher dose of 100 μg mL^{-1}, 60% cell viabilities

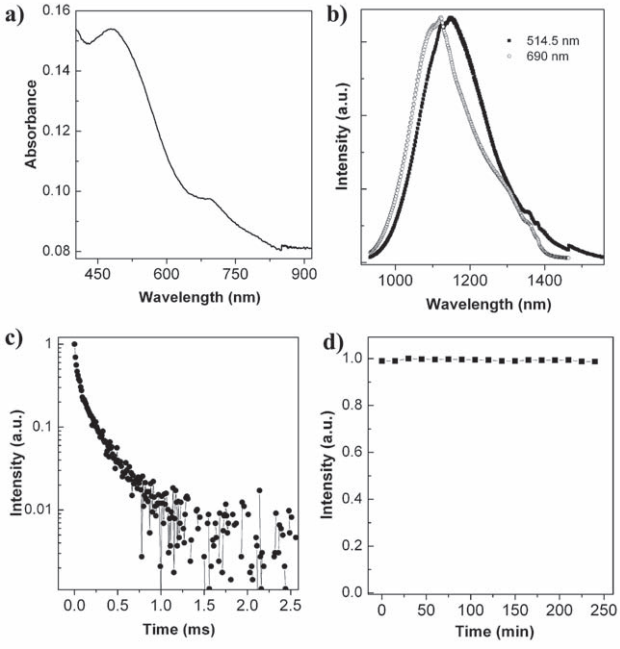

Figure 2. a) Absorption spectrum of the core/shell NPs. b) NIR PL spectra of the core/shell NPs in PBS solution, which were excited by the 514.5 nm line of an Ar^+ laser and 690 nm light of a laser diode (LD). c) Decay curve of the core/shell NPs in PBS solution. d) Photostability evaluation of the core/shell NPs dispersed in a polyvinylpyrrolidone (PVP) film. The excitation power and spot diameter are 410 mW and 1 mm, respectively.

NANO MICRO small

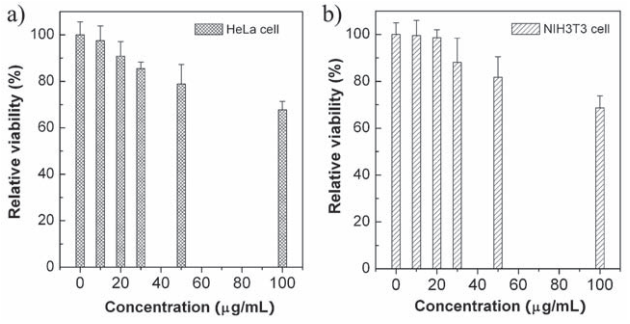

Figure 3. Viability of a) HeLa and b) NIH3T3 cells after 24 h of exposure to increasing doses of silica-coated Bi-AS-NPs, as evaluated with the MTT assay. Values are the mean standard deviation from four independent experiments.

can be maintained. The relatively low cytotoxicity of these NPs further indicates that they can be used for biomedical applications.

As is known, in living tissue the total photon attenuation is the sum of attenuation due to absorbance and scattering. Recent work carried out by Lim and colleagues revealed that NIR fluorophores with emission in the 1000–1400 nm range have higher tissue penetration than those near 800 nm, by considering the wavelength-dependent scattering by tissue.[1a,5a] The NPs shown here provide a unique way in which to probe this advantageous emission region. To further explore the potential of these NPs for deep-tissue imaging, we then performed in vivo NIR PL imaging in mice. A solution (100 μL, 1.0 mg mL^{-1}) was injected subcutaneously in the neck region of a mouse. During in vivo experiments, NIR excitation was achieved with a 690 nm continuous-wave laser (0.8 mW mm^{-2}). A long-pass filter (Schott, RG 1000) was used for imaging and the images had an identical exposure time (6 min). The false-color coded image in **Figure 4**a shows that mouse tissue shows weak autofluorescence. The NIR PL image was taken 30 min after hypodermic injection (Figure 4b). The NIR signal assigned to the emission of BiRIACs is extremely strong in the NIR region beyond 1 μm relative to the autofluorescence. Given that the NIR-extended CCD camera (Hamamatsu, digital camera ORCA-R^2) can only detect PL signals below 1100 nm and has low sensitivity from 1000 to 1100 nm, and that our NPs emit in a wide NIR range, it is believed that the use of a highly efficient InGaAs camera could decrease the exposure time for taking images. The above result indicates that these NPs have great potential for deep-tissue imaging.

It is well known that fluorescence lifetime imaging microscopy (FLIM) is a powerful tool for producing an image based on the differences in the exponential decay rate of the fluorescence from a sample. In such a case, the lifetime of the fluorophore signal, rather than its intensity, is used to create the image, which has the advantage of minimizing the effect of photon scattering in thick layers of sample. In general, most biological tissues exhibit characteristic decay times ranging from picoseconds to nanoseconds.[15,16] As shown in Figure 2c, our core/shell NP has a characteristic lifetime of hundreds of microseconds, which suggests that it is a suitable candidate for FLIM.

Next, we investigated the possibility of FLIM using these long-lived NPs. One mouse was injected hypodermically near the neck area with 50 μL solution. The 650 nm light (5 ns width, 20 Hz), with a power of ≈0.3 mW, from an optical parametric oscillator pumped by the third harmonic of a Nd:YAG laser was focused on the injection position. **Figure 5**a,b show the PL decays monitored at 1110, 1200, and 1300 nm before and after NP injection, respectively. It is obvious that the animal tissues show a rather short lifetime (<1 μs; Figure 5a). The in vivo PL decay transients were found to be nonexponential at all emission wavelengths (Figure 5b), and consisted of fast and slow components. The fast initial decays are attributed to the contribution of the tissue autofluorescence and the slow ones to that of the NPs (Supporting Information, Figure S6). These initial data provide strong evidence that these NPs are sufficient for in vivo FLIM in the wide NIR region. It is necessary to point out that, in contrast to the nanosecond- or even picosecond-level lifetime of semiconductor QDs and organic dyes, which were taken by using expensive picosecond or femtosecond lasers as excitation sources,[15,16] the longer lifetime of our NPs greatly relaxes the requirement of excitation sources for the FLIM measurement (Supporting Information, in vivo decay curve measurement).

In summary, silica-coated, bismuth-doped aluminosilicate NPs are introduced as a new type of nanosized NIR PL biolabel. The material has several important features, including facile synthesis, broad absorption bands from the visible to NIR region, highly efficient long-lived PL covering the second biological window, rather high photostability, and relatively low cytotoxicity. These properties give the NPs great potential for NIR PL imaging. Furthermore, not only in vivo PL bioimaging but also in vivo PL decays have been successfully tested in living mice as a proof of the concept. Taking all these aspects together, this nanocomposite might be a promising alternative to existing NIR luminescent nanomaterials for bioimaging.

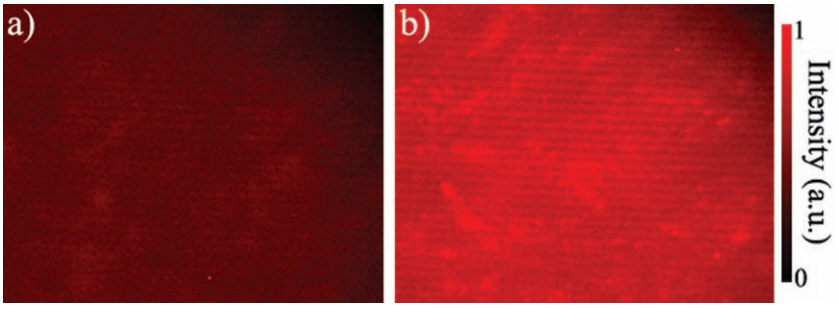

Figure 4. In vivo NIR PL imaging of a mouse a) before and b) after injection of NPs. Intensities are coded in false color, with bright red as the highest value. One mouse was injected subcutaneously in the neck region with a 100 μL solution. A microscope equipped with a NIR-extended digital camera (Hamamatsu, digital camera ORCA-R^2) was used for NIR fluorescence imaging. A 690 nm LD was externally mounted to provide epi-illumination of the mouse.

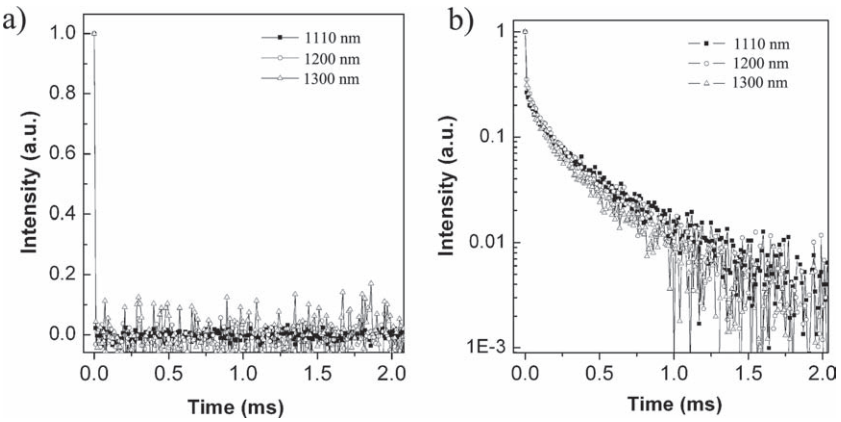

Figure 5. PL decay curves at 1110, 1200, and 1300 nm a) before and b) after injection of NPs. One mouse was injected subcutaneously in the neck region with 50 μL solution, and 650 nm light (5 ns width, 20 Hz) was focused on the injection position. The excitation power was around 0.3 mW.

Experimental Section

Synthesis: Zeolite NPs used for this experiment were synthesized by a modification of the approach developed by Mintova et al. and Fan et al.[17] In brief, silica sol (Sigma–Aldrich, Ludox SM-30 colloidal silica), tetramethylammonium hydroxide solution (Sigma–Aldrich, 25 wt% in H_2O), aluminum isopropoxide (Wako Pure Chemical Industries), and deionized water were mixed according to a mass ratio of 13.33:26.74:6.26:39.01. The mixture was stirred for about 15 min and then sonicated for 20 min. After ageing for 24 h at room temperature, the clear solution was transferred to a Teflon-lined stainless steel autoclave and kept at 100 °C for 48 h. The obtained zeolite NPs were carefully washed with deionized water three times by repeated dispersion–ultrasonication–centrifugation (14 000 rpm, 30 min), and finally dried at 90 °C in air. To remove the template, the sample was then thermally treated at 580 °C over 12 h in air. After that, the zeolite NPs were stirred in a 6.9 mM aqueous solution of Bi^{3+} prepared from $Bi(NO_3)_3{\cdot}5H_2O$ at 80 °C for 7 h to exchange the Na ions with Bi^{3+} ions. The products were removed by centrifugation, then washed with deionized water and dried in air at 80 °C. Aluminosilicate amorphous NPs could be obtained after annealing the Bi^{3+}-exchanged sample at 870 °C for 15 min in an Ar atmosphere. The coating of aluminosilicate NPs was realized by a Stöber method.[18] The NPs (600 mg) dissolved in deionized water (60 mL) were added to a mixture of ethanol (120 mL, 99.9%) and NH_4OH (3 mL, 28 wt%). After 20 min of ultrasonication, TEOS (0.5 mL)was added dropwise and the mixture was stirred for 60 min. The suspension was centrifuged (14 000 rpm, 10 min) and washed with ethanol five times. The precipitates were dried and annealed at 300 °C for 2 h in air.

Characterization: The products were characterized by X-ray diffraction (Rigaku-RINT Ultima3, λ = 1.54056 Å). The morphologies of the prepared products were characterized by TEM (JEOL, JSM-2100) at an accelerating voltage of 200 kV. Bismuth concentrations were measured by EDS. The atomic ratio for Bi-doped aluminosilicate NPs was determined to be around 2%. Samples were dispersed in Milli-Q water at a mass ratio of 10^{-5} g NPs to 1 g water, and the zeta potential of the core/shell NPs was measured using a LEZA-600 laser electrophoresis zeta-potential analyzer. PL excitation spectra were obtained at room temperature by a NIR PL spectrophotometer (Bunkoh-Keiki Co. Ltd., Tokyo, Japan) equipped with an InGaAs detector (Model 5851–13, Hamamatsu Photonics, Japan). The absorption spectrum was measured by a Jasco V-570 UV–vis–NIR spectrophotometer. NIR PL measurements were carried out at room temperature with excitation by the 514.5 nm line of an Ar^+ laser and 690 nm light from an LD (FC-690, Changchun New Industries Optoelectronics Tech. Co. Ltd., China). The signal was analyzed by a single-grating monochromator and detected by a liquid-nitrogen-cooled InGaAs detector (Princeton Instruments, USA). To evaluate the photostability property of NPs, we immobilized them in a PVP film, which was prepared on a pure silica substrate by spin coating. The film was continuously exposed to 690 nm laser excitation (410 mW; spot diameter: 1 mm). For all PL spectra, the spectral response of the detection system was corrected by the reference spectrum of a standard tungsten lamp. Time-resolved luminescence measurements were performed by detecting the modulated luminescence signal with a photomultiplier tube (Hamamatsu, R5509-72), and then analyzing the signal with a photon-counting multichannel scaler. The excitation source for the time-resolved PL measurements was the 514.5 nm light (5 ns width, 20 Hz) from an optical parametric oscillator pumped by the third harmonic of a Nd:YAG laser. The effective lifetimes τ_{eff} were calculated by using Origin 7.5 software based on Equation (1):

$$\tau_{\text{eff}-\text{NPs}} = \frac{\int_0^\infty t\,I(t)\,\mathrm{d}t}{\int_0^\infty I(t)\,\mathrm{d}t} \quad (1)$$

The PL *QE* was evaluated by a modified method reported in reference [10a]. Assuming that the radiative lifetime of BiRIACs is same in bismuth-doped NPs and glass (see Supporting Information, Figure S5), the *QE*s for the NPs can be estimated based on Equation (2):

$$\mathrm{QE}_{\mathrm{NPs}} = \mathrm{QE}_{\mathrm{Glass}} \times \frac{\tau_{\mathrm{eff-NPs}}}{\tau_{\mathrm{eff-Glass}}} \quad (2)$$

where QE_{NPs} and QE_{Glass} denote the *QE*s of SiO_2-coated Bi-AS-NPs and glass, respectively, while $\tau_{eff-NPs}$ and $\tau_{eff-Glass}$ denote the effective lifetime at 1145 nm taken at 300 K for NPs and glass, respectively. QE_{Glass} was determined to be 28.8% and the calculated QE_{NPs} is 14.6%.

Supporting Information

Supporting Information is available from the Wiley Online Library or from the author.

Acknowledgements

H.-T. S. is grateful for the funding support from the International Center for Young Scientists, National Institute for Materials Science, Japan (grant no. 215114).

[1] a) Y. T. Lim, S. Kim, A. Nakayama, N. E. Stott, M. G. Bawendi, J. V. Frangioni, *Mol. Imaging* **2003**, *2*, 50; b) J. V. Frangioni, *Curr. Opin. Chem. Biol.* **2003**, *7*, 626; c) A. Becker, C. Hessenius, K. Licha, B. Ebert, U. Sukowski, W. Semmler, B. Wiedenmann, C. Grötzinger, *Nat. Biotechnol.* **2001**, *19*, 321; d) H. Choi, W. Liu, F. Liu, K. Nasr, P. Misra, M. Bawendi, J. V. Frangioni, *Nat. Nanotechnol.* **2010**, *5*, 42.

[2] a) P. Cherukuri, S. M. Bachilo, S. H. Litovsky, R. B. Weisman, *J. Am. Chem. Soc.* **2004**, *126*, 15638; b) X. H. Gao, Y. Cui, R. M. Levenson, L. Chung, S. M. Nie, *Nat. Biotechnol.* **2004**, *22*, 969; c) S. Kim, Y. Lim, E. Soltesz, A. Grand, J. Lee, A. Nakayama, J. Parker, T. Mihaljevic, R. G. Laurence, D. Dor, L. Cohn, M. Bawendi, J. V. Frangioni, *Nat. Biotechnol.* **2004**, *22*, 93; d) X. H. Gao, L. Yang, J. Petros, F. Marshall, J. Simons, S. M. Nie, *Curr. Opin. Chem. Biol.* **2005**, *16*, 63; e) B. Hennequin, L. Turyanska, T. Ben, A. Beltran, S. Molina, M. Li, S. Mann, A. Patane, N. Thomas, *Adv. Mater.* **2008**, *20*, 3592.

[3] a) U. Resch-Genger, M. Grabolle, S. Cavaliere-Jaricot, R. Nitschke, T. Nann, *Nat. Methods* **2008**, *5*, 763; b) E. Altınoğlu, T. Russin, J. Kaiser, B. Barth, P. Eklund, M. Kester, J. Adair, *ACS Nano* **2008**, *2*, 2075; c) D. L. Shi, H. Cho, Y. Chen, H. Xu, H. Gu, J. Lian, W. Wang, G. Liu, C. Huth, L. Wang, R. Ewing, S. Budko, G. Pauletti, Z. Dong, *Adv. Mater.* **2009**, *21*, 2170; d) D. L. Shi, *Adv. Funct. Mater.* **2009**, *19*, 3356.

[4] a) S. Santra, P. Zhang, K. Wang, R. Tapec, W. H. Tan, *Anal. Chem.* **2001**, *73*, 4988; b) X. Zhao, R. Bagwe, W. H. Tan, *Adv. Mater.* **2004**, *16*, 173; c) L. Wang, W. H. Tan, *Nano Lett.* **2006**, *6*, 84; d) C. Lee, S. Cheng, Y. Wang, Y. Chen, N. Chen, J. Souris, C. Chen, C. Mou, C. Yang, L. Lo, *Adv. Funct. Mater.* **2009**, *19*, 215.

[5] a) K. Welsher, Z. Liu, S. Sherlock, J. Robinson, Z. Chen, D. Daranciang, H. J. Dai, *Nat. Nanotechnol.* **2007**, *2*, 47; b) J. Park, L. Gu, G. Maltzahn, E. Ruoslahti, S. N. Bhatia, M. J. Sailor, *Nat. Mater.* **2009**, *8*, 331; c) R. Kumar, M. Nyk, T. Y. Ohulchanskyy, C. A. Flask, P. N. Prasad, *Adv. Funct. Mater.* **2009**, *19*, 853; d) X. Yu, L. Chen, M. Li, M. Xie, L. Zhou, Y. Li, Q. Wang, *Adv. Mater.* **2008**, *20*, 4118; e) M. Nyk, R. Kumar, T. Y. Ohulchanskyy, E. J. Bergey, P. N. Prasad, *Nano Lett.* **2008**, *8*, 3834; f) K. Park, S. Lee, E. Kang, K. Kim, K. Choi, I. Kwon, *Adv. Funct. Mater.* **2009**, *19*, 1553.

[6] N. Mohan, Y. Tzeng, L. Yang, Y. Chen, Y. Hui, C. Fang, H. Chang, *Adv. Mater.* **2009**, *22*, 843.

[7] X. G. Peng, *Nat. Mater.* **2006**, *5*, 923.

[8] a) J. R. Partington, *A History of Chemistry*, Macmillan, London **1961**; b) P. Sadler, H. Li, H. Sun, *Coordin. Chem. Rev.* **1999**, *185–186*, 689; c) A. Slikkerveer, F. A. de Wolff, *Med. Toxicol. Adverse Drug Exp.* **1989**, *4*, 303; d) H. Menge, M. Gregor, B. Brosius, R. Hopert, A. Lang, *Eur. J. Gastroenterol. Hepatol.* **1994**, *4*, 41.

[9] Summary report of bismuth subnitrate, subcarbonate, subgallate, and subsalicylate from the Committee for Veterinary Medical Products (CVMP), http://www.ema.europa.eu/pdfs/vet/mrls/020197en.pdf (accessed January 2010).

[10] a) H. Sun, A. Hosokawa, Y. Miwa, F. Shimaoka, M. Fujii, M. Mizuhata, S. Hayashi, S. Deki, *Adv. Mater.* **2009**, *21*, 3694; b) S. Zhou, N. Jiang, B. Zhu, H. Yang, S. Ye, G. Lakshminarayana, J. Hao, J. Qiu, *Adv. Funct. Mater.* **2008**, *18*, 1407; c) Y. Fujimoto, M. Nakatsuka, *Jpn. J. Appl. Phys.* **2001**, *40*, L279; d) H. Sun, Y. Miwa, F. Shimaoka, M. Fujii, A. Hosokawa, M. Mizuhata, S. Hayashi, S. Deki, *Opt. Lett.* **2009**, *34*, 1219; e) H. Sun, M. Fujii, Y. Sakka, Z. Bai, N. Shirahata, L. Zhang, Y. Miwa, H. Gao, *Opt. Lett.* **2010**, *35*, 1743; f) H. Sun, T. Hasegawa, M. Fujii, F. Shimaoka, Z. Bai, M. Mizuhata, S. Hayashi, S. Deki, *Opt. Express* **2009**, *17*, 6239.

[11] H. Peiper in *Zeolite: Nature's Heavy Metal Detoxifier*, New Century Publishing, Indianapolis **2006**, pp. 1–44.

[12] Y. S. Li, J. L. Shi, Z. Hua, H. Chen, M. Ruan, D. Yan, *Nano Lett.* **2003**, *3*, 609.

[13] K. Hayakawa, Y. Mouri, T. Maeda, I. Satake, M. Sato, *Colloid Polym. Sci.* **2000**, *278*, 553.

[14] a) B. Weon, J. Je, J. Lee, *Appl. Phys. A* **2007**, *89*, 1029; b) A. Kigel, M. Brumer, G. Maikov, A. Sashchiuk, E. Lifshitz, *Superlattices Microstruct.* **2009**, *46*, 272; c) G. Giraud, H. Schulze, T. Bachmann, C. Campbell, A. Mount, P. Ghazal, M. Khondoker, A. Ross, S. Ember, I. Ciani, C. Tlili, A. Walton, J. Terry, J. Crain, *Int. J. Mol. Sci.* **2009**, *10*, 1930.

[15] K. Konig, *J. Microsc.* **2000**, *200*, 83.

[16] D. Elson, J. Requejo-Isidro, I. Munro, F. Reavell, J. Siegel, K. Suhling, P. Tadrous, R. Benninger, P. Lanigan, J. McGinty, C. Talbot, B. Treanor, S. Webb, A. Sandison, A. Wallace, D. Davis, J. Lever, M. Neil, D. Phillips, G. Stamp, P. French, *Photochem. Photobiol. Sci.* **2004**, *3*, 795.

[17] a) S. Mintova, N. Olson, T. Bein, *Angew. Chem. Int. Ed.* **1999**, *38*, 3201; b) W. Fan, S. Shirato, F. Gao, M. Ogura, T. Okubo, *Microporous Mesoporous Mater.* **2006**, *89*, 227.

[18] W. Stöber, A. Fink, E. J. Bohn, *J. Colloid Interface Sci.* **1968**, *26*, 62.

Received: June 14, 2010
Published online: December 9, 2010

